ORIGINAL ARTICLE

Mutations in *DSTYK* and Dominant Urinary Tract Malformations

S. Sanna-Cherchi, R.V. Sampogna, N. Papeta, K.E. Burgess, S.N. Nees, B.J. Perry,
M. Choi, M. Bodria, Y. Liu, P.L. Weng, V.J. Lozanovski, M. Verbitsky, F. Lugani,
R. Sterken, N. Paragas, G. Caridi, A. Carrea, M. Dagnino, A. Materna-Kiryluk,
G. Santamaria, C. Murtas, N. Ristoska-Bojkovska, C. Izzi, N. Kacak, B. Bianco,
S. Giberti, M. Gigante, G. Piaggio, L. Gesualdo, D. Kosuljandic Vukic,
K. Vukojevic, M. Saraga-Babic, M. Saraga, Z. Gucev, L. Allegri, A. Latos-Bielenska,
D. Casu, M. State, F. Scolari, R. Ravazzolo, K. Kiryluk, Q. Al-Awqati, V.D. D'Agati,
I.A. Drummond, V. Tasic, R.P. Lifton, G.M. Ghiggeri, and A.G. Gharavi

ABSTRACT

BACKGROUND

Congenital abnormalities of the kidney and the urinary tract are the most common cause of pediatric kidney failure. These disorders are highly heterogeneous, and the etiologic factors are poorly understood.

METHODS

We performed genomewide linkage analysis and whole-exome sequencing in a family with an autosomal dominant form of congenital abnormalities of the kidney or urinary tract (seven affected family members). We also performed a sequence analysis in 311 unrelated patients, as well as histologic and functional studies.

RESULTS

Linkage analysis identified five regions of the genome that were shared among all affected family members. Exome sequencing identified a single, rare, deleterious variant within these linkage intervals, a heterozygous splice-site mutation in the dual serine–threonine and tyrosine protein kinase gene (*DSTYK*). This variant, which resulted in aberrant splicing of messenger RNA, was present in all affected family members. Additional, independent *DSTYK* mutations, including nonsense and splice-site mutations, were detected in 7 of 311 unrelated patients. DSTYK is highly expressed in the maturing epithelia of all major organs, localizing to cell membranes. Knockdown in zebrafish resulted in developmental defects in multiple organs, which suggested loss of fibroblast growth factor (FGF) signaling. Consistent with this finding is the observation that DSTYK colocalizes with FGF receptors in the ureteric bud and metanephric mesenchyme. *DSTYK* knockdown in human embryonic kidney cells inhibited FGF-stimulated phosphorylation of extracellular-signal-regulated kinase (ERK), the principal signal downstream of receptor tyrosine kinases.

CONCLUSIONS

We detected independent *DSTYK* mutations in 2.3% of patients with congenital abnormalities of the kidney or urinary tract, a finding that suggests that DSTYK is a major determinant of human urinary tract development, downstream of FGF signaling. (Funded by the National Institutes of Health and others.)

CONGENITAL MALFORMATIONS OF THE kidney and urinary tract contribute to 23% of birth defects[1,2] and account for 40 to 50% of pediatric cases and 7% of adult cases of end-stage renal disease (ESRD) worldwide.[3,4] These disorders are genetically heterogeneous and encompass a wide range of anatomical defects, such as renal agenesis, renal hypodysplasia, ureteropelvic junction obstruction, or vesicoureteral reflux.[5] Mutations in genes that cause syndromic disorders, such as *HNF1B* and *PAX2* mutations, are detected in only 5 to 10% of cases.[6,7] Familial forms of nonsyndromic disease have been reported, further supporting genetic determination[8,9]; however, owing to locus heterogeneity and small pedigree size, the genetic cause of most familial or sporadic cases remains unknown.

We studied a family with an autosomal dominant form of congenital abnormalities of the kidney and urinary tract (Fig. 1A; and Table S1 in the Supplementary Appendix, available with the full text of this article at NEJM.org).[8] Seven family members were classified as affected on the basis of the presence of a solitary kidney, renal hypodysplasia, ureteropelvic junction obstruction, or vesicoureteral reflux, as documented by means of imaging studies. The mean age at diagnosis was 12 years (range, 1 to 37). Three family members (members 7, 8, and 13), all with ureteropelvic junction obstruction, had ESRD at a young age (at 8, 10, and 23 years of age, respectively), without other known causes of renal failure, such as diabetes mellitus or uncontrolled hypertension. Epilepsy developed in these three persons during their third decade of life. The other affected family members did not have evidence of renal dysfunction at the last follow-up visit. Seven family members were classified as unaffected on the basis of normal ultrasonographic studies of the abdomen and normal renal function, and six were classified as having an unknown phenotype, owing to unavailable or indeterminate ultrasonographic studies.

A series of 311 patients with congenital abnormalities of the kidney and urinary tract was studied to identify independent mutations. Genetic and clinical data for 7 of these patients (5 of whom had congenital obstructive uropathy) are shown in Table 1 and Figure 1.

METHODS

GENOTYPING AND SEQUENCING

After genomewide genotyping, we conducted a genomewide analysis of linkage, under an autosomal dominant mode of inheritance, with assignment of phenotype only to affected persons (affected-only analysis). Rare copy-number variants were excluded with the use of HumanHap 650Y Genotyping BeadChips (Illumina). Whole-exome sequencing and analysis were performed as previously described[10,11] in two members of the family (members 13 and 19).

We performed Sanger sequencing of *DSTYK* to validate exome data and detect independent mutations in 311 unrelated patients with congenital abnormalities of the kidney and urinary tract and in 384 healthy European controls matched to patients with *DSTYK* mutations according to self-reported ethnic group; 96 of these controls were also matched according to recruitment site. Coding exons and flanking introns of *HNF1B*, *PAX2*, and *EYA1* were sequenced in the 7 patients carrying *DSTYK* mutations. We determined allele frequencies with the use of public databases, scores from Polymorphism Phenotyping, version 2 (PolyPhen-2), and alignment in 22 mammalian species.

Written informed consent was obtained from all the participants. The study was approved by the institutional review board at each participating site. All the authors vouch for the accuracy and completeness of the data and for the fidelity of the study to the protocol.

LYMPHOCYTE IMMORTALIZATION AND DNA ANALYSIS

We generated lymphoblastoid cell lines from 17 family members. Total RNA was isolated, complementary DNA (cDNA) was generated, and Sanger sequencing was performed on the cDNA with the use of primers spanning the exon 2 and 3 boundaries.

IMMUNOHISTOCHEMICAL AND IMMUNOFLUORESCENCE TESTING

DSTYK expression was examined in adult and embryonic mouse organs (embryonic day 15.5 to 18.5) and in a kidney and ureter from a pediatric donor (3 months of age; International Institute
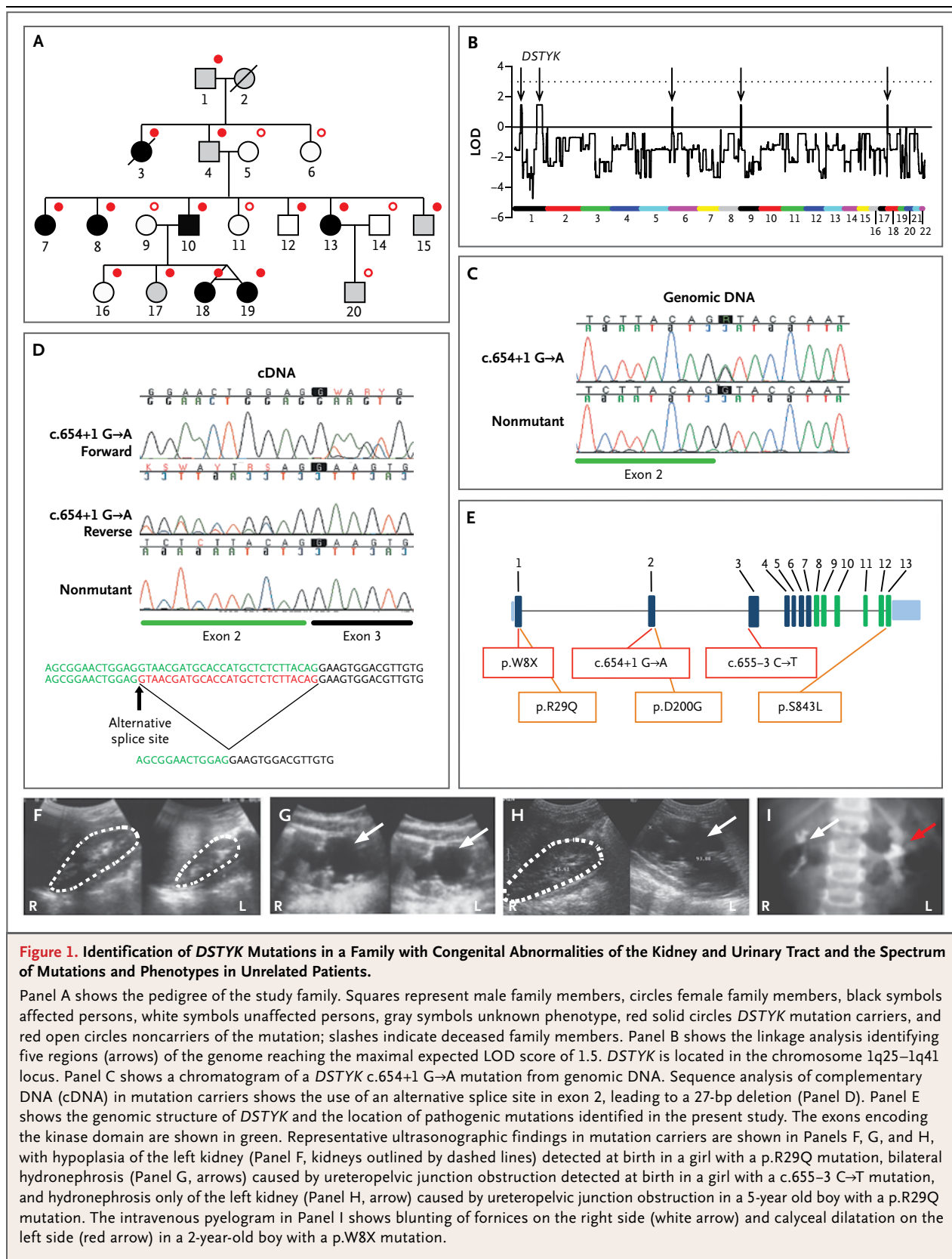
Figure 1. Identification of *DSTYK* Mutations in a Family with Congenital Abnormalities of the Kidney and Urinary Tract and the Spectrum of Mutations and Phenotypes in Unrelated Patients.

Panel A shows the pedigree of the study family. Squares represent male family members, circles female family members, black symbols affected persons, white symbols unaffected persons, gray symbols unknown phenotype, red solid circles *DSTYK* mutation carriers, and red open circles noncarriers of the mutation; slashes indicate deceased family members. Panel B shows the linkage analysis identifying five regions (arrows) of the genome reaching the maximal expected LOD score of 1.5. *DSTYK* is located in the chromosome 1q25–1q41 locus. Panel C shows a chromatogram of a *DSTYK* c.654+1 G→A mutation from genomic DNA. Sequence analysis of complementary DNA (cDNA) in mutation carriers shows the use of an alternative splice site in exon 2, leading to a 27-bp deletion (Panel D). Panel E shows the genomic structure of *DSTYK* and the location of pathogenic mutations identified in the present study. The exons encoding the kinase domain are shown in green. Representative ultrasonographic findings in mutation carriers are shown in Panels F, G, and H, with hypoplasia of the left kidney (Panel F, kidneys outlined by dashed lines) detected at birth in a girl with a p.R29Q mutation, bilateral hydronephrosis (Panel G, arrows) caused by ureteropelvic junction obstruction detected at birth in a girl with a c.655–3 C→T mutation, and hydronephrosis only of the left kidney (Panel H, arrow) caused by ureteropelvic junction obstruction in a 5-year old boy with a p.R29Q mutation. The intravenous pyelogram in Panel I shows blunting of fornices on the right side (white arrow) and calyceal dilatation on the left side (red arrow) in a 2-year-old boy with a p.W8X mutation.

Table 1. Spectrum of *DSTYK* Mutations and Associated Phenotypes.*

Variant	Consequence	PolyPhen-2 Prediction (Score)†	Ancestry‡	Sex	Age at Diagnosis	Phenotype	Familial or Sporadic Disease	Chronic Renal Failure or Dialysis	Extraurinary Tract Condition
Splice-site or truncating mutation									
c.654+1 G→A (in seven members of the study family)§	p.V210_Q218del	NA	Italian	M and F	1–37 yr	RHD, UPJO, and VUR	Familial	Yes (members 7, 8, and 13)	Epilepsy (members 7, 8, and 13)
c.24G→A	p.W8X	NA	Macedonian	M	2 yr	UPJO	Sporadic	No	Hemangioma, ataxia (resolved), and hearing loss
c.655–3 C→T (in two siblings from another family)¶	—	NA	Italian	F	At birth	UPJO	Familial	No	Hypercalciuria
Missense mutation									
c.86G→A	p.R29Q	Probably damaging (0.997)	Albanian	M	5 yr	UPJO	Sporadic	No	—
c.86G→A	p.R29Q	Probably damaging (0.997)	Italian	M	Prenatal	RHD	Sporadic	Yes	—
c.86G→A	p.R29Q	Probably damaging (0.997)	Albanian	F	At birth	RHD	Sporadic	No	Congenital adrenal hyperplasia
c.599A→G	p.D200G	Probably damaging (0.992)	Italian	M	At birth	UPJO	Sporadic	No	Hearing loss
c.2528 C→T	p.S843L	Possibly damaging (0.741)	Croatian	M	5 mo	CHN	Sporadic	Yes	Factor VII deficiency and hypercalciuria

* The protein and complementary DNA annotations are based on National Center for Biotechnology Information reference sequence numbers NP_056190.1 and NM_015375.2, respectively. All variants in this table were absent in both the Single Nucleotide Polymorphism database for build 137 and the exome variant server and were not detected in 384 European controls. CHN denotes congenital hydronephrosis, NA not applicable, RHD renal hypodysplasia, UPJO ureteropelvic junction obstruction, and VUR vesicoureteral reflux.
† Scores from Polymorphism Phenotyping, version 2 (PolyPhen-2), indicate the probability of the mutation causing damage.
‡ Ancestry was self-reported and confirmed by the investigator on the basis of the nationality and region of birth of the index patient and his or her parents and grandparents.
§ Detailed phenotypes of the seven affected family members are described in Table S1 in the Supplementary Appendix.
¶ This mutation was found in two siblings with obstructive uropathy; only one sibling was counted in the group of 311 unrelated patients. The c.655–3 C→T variant is predicted to decrease the consensus values for the canonical splice site from 96.68 to 89, corresponding to a −7.95% variation (Human Splicing Finder; www.umd.be/HSF/).

for the Advancement of Medicine). Immunohisto-chemical testing was performed with the use of anti-DSTYK antibody (also called anti-RIP5 antibody; Universal Protein Resource Knowledgebase accession number, Q6XUX3; catalogue number, sc-162109; Santa Cruz Biotechnology) on paraffin-embedded tissues with the use of heat-induced antigen retrieval. Immunofluorescence testing was performed with the use of the following antibodies: anti-RIP5 antibody, antibodies to fibroblast growth factor (FGF) receptors 1 and 2 (anti-FGFR1 and anti-FGFR2 antibodies, respectively), anti–aquaporin-2 antibody, and anti–E-cadherin antibody (see the Supplementary Appendix).

ZEBRAFISH MORPHOLINO KNOCKDOWN

Morpholino oligomers were designed to block the zebrafish *dstyk* (National Center for Biotechnology Information reference sequence number, NM_205627.2) exon 9 splice donor and to truncate or delete the ATP-binding kinase domain. Morpholino injections were also performed in tumor-suppressor protein (p53)–mutant homozygotes[12] to control for nonspecific antisense effects.

SMALL INTERFERING RNA KNOCKDOWN AND WESTERN BLOTTING

Human embryonic kidney 293T cells were grown with the use of standard procedures. The cells were transfected with a mixture of *DSTYK* small interfering RNAs (siRNAs; SMARTpool, Dharmacon); for a negative control, we used a pool of siRNA that was tested by the manufacturer for not interfering with any transcript. At 72 to 96 hours after transfection, the cells were starved in serum-free medium and treated with FGF. Blotting was performed as above with the use of goat anti-RIP5 and rabbit anti-FGFR2 antibodies; mouse anti–glyceraldehyde-3-phosphate dehydrogenase antibody; rabbit anti–phosphorylated extracellular-signal-regulated kinase (pERK) 1 and 2 and anti–extracellular-signal-regulated kinase (ERK) 1 and 2 antibodies; and horseradish-peroxidase–labeled sheep antimouse, donkey antigoat, or donkey antirabbit antibody. Detailed methods are included in the Supplementary Appendix.

RESULTS

HETEROZYGOUS MUTATIONS IN *DSTYK*

Genomewide analysis of linkage with the use of an affected-only analysis identified five regions of the genome that were shared among all seven affected members (Fig. 1). These intervals collectively spanned 55.44 Mb (approximately 1.8%) of the genome, containing 645 protein-coding genes (Table S2 in the Supplementary Appendix). Analysis of copy-number variants in all affected persons excluded major genomic imbalances (data not shown).

Whole-exome sequencing, performed in members 13 and 19 of the study family (Fig. 1A) at an average depth of coverage of approximately 108 times per base, identified 14,943 single-nucleotide variants (SNVs) across the genome, including 709 SNVs that were absent in all public databases. Among these, 24 protein-altering variants were shared by these two patients (missense, nonsense, or splice-site variants) (Table S3 in the Supplementary Appendix). Only 2 of these 24 SNVs, both on chromosome 1q25–1q41, mapped to the linkage intervals.

Follow-up testing by means of Sanger sequencing detected both SNVs in all affected persons and the obligate carrier in the family. One of these SNVs (p.A111V in *TIMM17A*) was common among persons of Sardinian ancestry (minor allele frequency, 0.47). The other variant, a canonical splice-donor SNV at the first base after exon 2 (c.654+1 G→A) of *DSTYK*, encoding a dual serine–threonine and tyrosine kinase, was absent in 48 persons of Sardinian ancestry and 384 European controls (Fig. 1C). The *DSTYK* mutation was heterozygous in all affected persons, obligate carriers, and two apparently unaffected members (who were 44 and 20 years old at the last follow-up visit).

Sequence analysis of *DSTYK* cDNA from lymphoblastoid cell lines in 17 family members showed that all mutation carriers had a heterozygous 27-bp deletion resulting from the use of an alternative splice donor within the normal exon 2, which would result in an in-frame deletion of nine amino acids (VTMHHALLQ) in a domain that is highly conserved among mammals (Fig. 1, and Fig. S1 and S2 in the Supplementary Appendix).

We next searched for independent mutations in *DSTYK* in 311 additional patients with congenital abnormalities of the kidney and urinary tract. We identified a nonsense mutation (p.W8X) in a patient with ureteropelvic junction obstruction and early-onset ataxia, and a splice-site mutation (c.655–3 C→T) in two siblings affected by ureteropelvic junction obstruction. We also iden-

tified, in 5 other patients, three missense variants that occur at completely conserved positions in mammals and that were predicted to be damaging according to PolyPhen-2 (p.R29Q, p.D200G, and p.S843L). These five damaging variants were absent in all public databases and were also not detected in the 384 healthy European controls. Moreover, none of these patients carried deleterious structural variants[13] or point mutations in *HNF1B*, *PAX2*, or *EYA1*. The phenotypic spectrum associated with *DSTYK* mutations is described in Table 1 and shown in Figures 1F through 1I.

Thus, sequence analysis in an independent cohort of 311 unrelated patients with congenital abnormalities of the kidney and urinary tract identified five *DSTYK* mutations in 7 patients (2.3% of this independent cohort) (Table 1). As a comparison, the exome variant server (a database hosted by the National Heart, Lung, and Blood Institute that contains exome data for 6503 people) does not contain any *DSTYK* nonsense mutations or variants affecting the three canonical nucleotides flanking splice junctions. Only 0.3% of white persons (14 of 4300) in this database have rare damaging *DSTYK* missense variants affecting completely conserved positions in mammals (11 variants with a minor allele frequency of <0.001), indicating a significant excess burden of rare damaging variants among persons with congenital abnormalities of the kidney and urinary tract (7 of 311 affected persons [2.3%]; odds ratio, 7.1; P=0.0003 by Fisher's exact test).

UBIQUITOUS EXPRESSION OF DSTYK ON CELL MEMBRANES

DSTYK has a striking membrane-associated distribution in mesenchymal-derived cells of all major organs (Fig. S3 in the Supplementary Appendix). In the developing mouse kidney, it is expressed at low levels in the nephrogenic zone but is more highly expressed in maturing tubular epithelia, with the most prominent expression in the medulla and the papilla (Fig. S3G, S3H, and S3I in the Supplementary Appendix). In postnatal mouse and human pediatric kidneys, DSTYK is detected in the basolateral and apical membranes of all tubular epithelia (Fig. 2A through 2D, and Fig. S4 in the Supplementary Appendix). It has both a basolateral and a cytoplasmic distribution in the thin ascending limb of the loop of Henle and the distal convoluted tubule, but expression is restricted to apical and basolateral membranes in the collecting duct, including the principal and intercalated cells (Fig. 2A through 2D, and Fig. S5 in the Supplementary Appendix). DSTYK was also detected in all layers of transitional ureteric epithelium and in the ureteric smooth-muscle cells (Fig. 2D).

MORPHOLINO KNOCKDOWN IN ZEBRAFISH

To investigate the role of DSTYK in embryonic development, we performed knockdown of the orthologue in zebrafish. With maximal knockdown, embryos showed growth retardation, as evidenced by small fins, abnormal morphogenesis of the tail, and loss of heartbeat (Fig. S6 in the Supplementary Appendix); we also observed cloacal malformations that correspond to lower genitourinary defects in mammals and defects in jaw development, as well as specific loss of the median fin fold. Pericardial effusion was evident in 5-day-old morphant larvae, which was attributable to both heart and kidney failure. These data suggest an essential role of DSTYK in the development of major organs. The observed developmental defects resemble phenotypes produced by global loss of FGF signaling in zebrafish.[14-16]

COLOCALIZATION OF DSTYK AND FGF RECEPTORS AND EFFECT ON ERK PHOSPHORYLATION

In the developing mouse nephron (embryonic day 15.5), DSTYK colocalizes with cells that are E-cadherin–positive and those that are E-cadherin–negative, confirming its expression in both the metanephric mesenchyme and the ureteric bud (Fig. 2G and 2H). DSTYK localization to the cell membrane in the metanephric mesenchyme and ureteric bud highly parallels the known expression pattern of FGF receptors. Joint immunostaining confirmed that DSTYK colocalizes with both FGFR1 and FGFR2 in the ureteric bud and comma-shaped bodies (Fig. 2G and 2H, and Fig. S7 in the Supplementary Appendix). Colocalization with FGFR2 was also evident in distal tubular cells in the adult renal medulla and papilla (Fig. S8 in the Supplementary Appendix). Punctate DSTYK staining was seen at apical cell–cell junctions lining the ureteric-bud epithelia (Fig. S9 and S10 in the Supplementary Appendix).

On activation, FGF receptors trigger cytoplasmic protein kinases, resulting in ERK phosphorylation, which is the main effector of FGF-induced transcriptional activity.[17,18] Because *DSTYK* encodes a kinase and colocalizes with FGFR1 and FGFR2, we hypothesized that DSTYK acts as a positive regulator of FGF-mediated signaling in
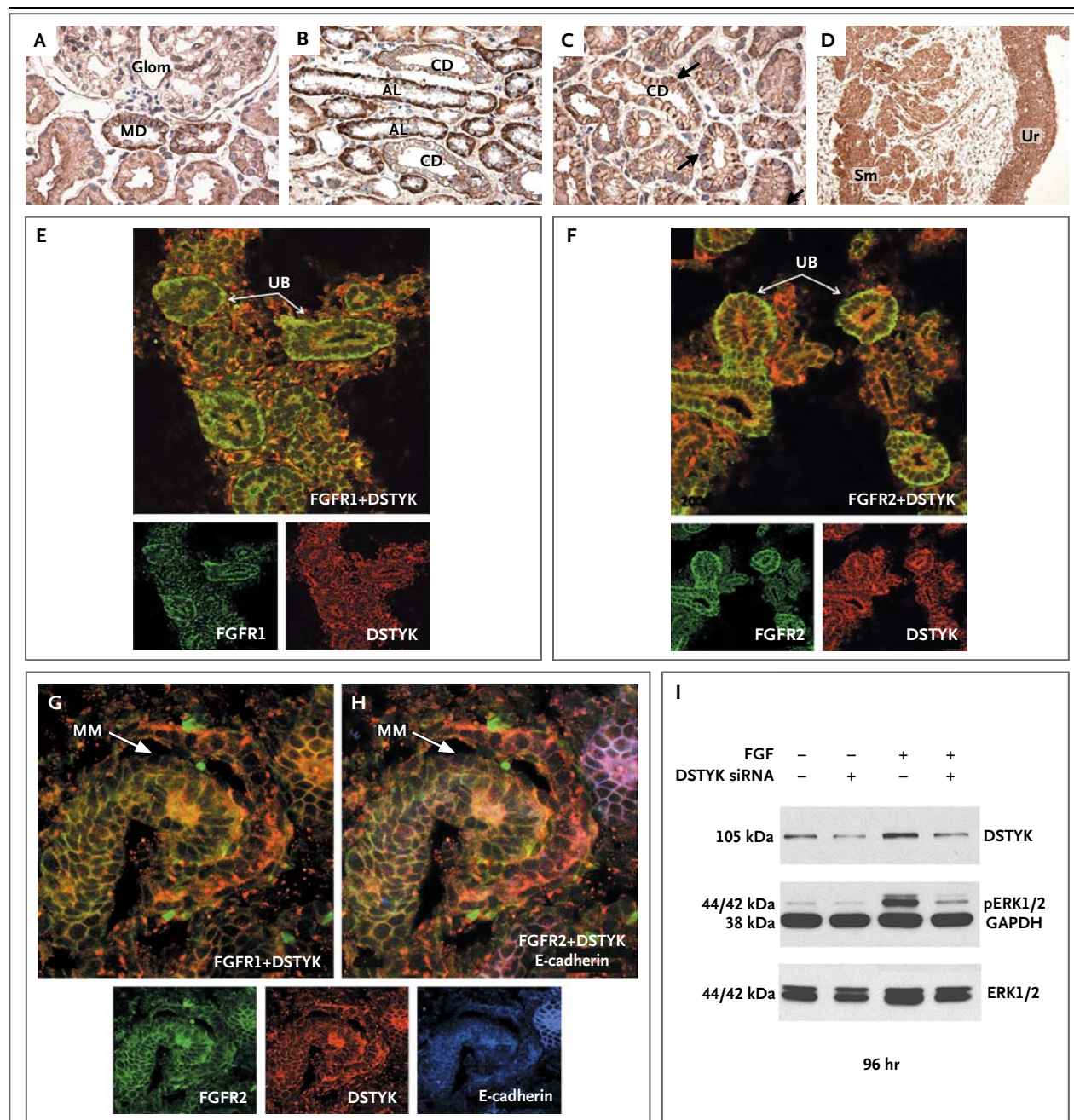
Figure 2. DSTYK Expression in the Human and Mouse Urinary Tract and Small Interfering RNA (siRNA) Knockdown Studies.

Panels A through D show DSTYK expression in the kidney and ureter of a 3-month-old child. Panel A shows the glomerulus (Glom) and macula densa (MD). Panel B shows the renal cortex with ascending limbs of loop of Henle (AL) and collecting ducts (CD). Panel C shows the CD in the renal medulla, with punctate staining at the basolateral side (arrows). Panel D shows the smooth-muscle layer (Sm) and urothelium (Ur) of the ureter. Panels E through H show DSTYK colocalizing with fibroblast growth factor (FGF) receptors. Immunofluorescence analysis in a developing murine kidney (embryonic day 15.5) shows DSTYK (red) colocalization with FGF receptor 1 (FGFR1; green) (Panel E), FGF receptor 2 (FGFR2; green) (Panels F, G, and H) and E-cadherin (Panel H; blue). In Panel I, DSTYK knockdown is shown to inhibit FGF-mediated phosphorylation of extracellular-signal-regulated kinase 1 and 2 (ERK 1 and 2); siRNA knockdown of *DSTYK* in 293T cells starved in serum-free medium shows a significant reduction in the DSTYK level at 96 hours after knockdown. FGF stimulation significantly augments phosphorylated ERK (pERK 1 and 2), but *DSTYK* knockdown abrogates FGF-mediated ERK phosphorylation. Glyceraldehyde-3-phosphate dehydrogenase (GAPDH) was used as a loading control. MM denotes metanephric mesenchyme, and UB ureteric bud.

the kidney. To test this hypothesis, we performed siRNA knockdown of *DSTYK* in the human embryonic kidney-cell line 293T, which resulted in a reduction of up to 80% in transcript levels and a pronounced reduction of DSTYK protein levels within the first 96 hours after transfection (Fig. 2I, and Fig. S11 in the Supplementary Appendix). FGF stimulation augmented the levels of phosphorylated ERK (pERK) as expected, but siRNA silencing of *DSTYK* significantly prevented ERK phosphorylation (Fig. 2I). This effect was not mediated by a direct physical interaction of DSTYK with FGFR2 (Fig. S12 in the Supplementary Appendix). Combined with colocalization of DSTYK with FGFR1 and FGFR2, these data implicate DSTYK downstream of FGF signaling.

DISCUSSION

The development of the kidney and the urinary tract is orchestrated by a series of inductive signals between the metanephric mesenchyme and the ureteric bud, and any disruption of this reciprocal signaling results in developmental defects.[19-22] The diversity of signaling pathways in nephrogenesis explains the significant locus heterogeneity of congenital abnormalities of the kidney and urinary tract.[20] For example, in a recent study involving 522 patients with kidney malformations, we identified 72 distinct copy-number disorders in 87 patients, suggesting that virtually every patient may have a unique genetic diagnosis.[13]

In the current study, we identified independent mutations in *DSTYK* in 2.3% of patients with congenital abnormalities of the kidney and urinary tract. The identification of a heterozygous nonsense mutation suggests haploinsufficiency as a potential genetic mechanism, underscoring a critical role of *DSTYK* gene dosage in the development of the human urinary tract. Mutations were detected in patients with defects in the ureter and renal parenchyma, an observation that is consistent with DSTYK expression in the ureteric bud and metanephric mesenchyme. These findings show the effectiveness of exome sequencing for the elucidation of heterogeneous developmental traits with modest-sized pedigrees.

In humans, a total of 22 FGF ligands signal through four FGF receptors, conferring both complexity and redundancy to this pathway.[17,23] Different combinations of FGF ligands are expressed in the ureteric bud, metanephric mesenchyme, and renal stroma,[17] and a recessive *FGF20* mutation was recently reported in a family with renal agenesis.[21] FGFR1 and FGFR2 are responsible for most of the FGF signaling during nephrogenesis.[17,22,24] Engagement of the FGF receptor results in autophosphorylation and activation of the intracellular mitogen-activated protein kinase cascade, ultimately resulting in the production of pERK, the main effector of the FGF transcriptional program.[17,23]

Our data indicate that DSTYK is a positive regulator of ERK phosphorylation downstream of FGF-receptor activation. A previous study has suggested a role of DSTYK in the induction of apoptosis, a pathway also regulated by FGF signaling.[25] Additional studies will therefore be required to delineate the precise role of DSTYK in this signal-transduction cascade. Identification of other components of this pathway may elucidate additional forms of congenital abnormalities of the kidney and urinary tract in humans.

APPENDIX

The authors' full names and academic degrees are as follows: Simone Sanna-Cherchi, M.D., Rosemary V. Sampogna, M.D., Ph.D., Natalia Papeta, Ph.D., Katelyn E. Burgess, B.S., Shannon N. Nees, M.D., Brittany J. Perry, M.A., Murim Choi, Ph.D., Monica Bodria, M.D., Yan Liu, M.S., Patricia L. Weng, M.D., Vladimir J. Lozanovski, M.D., Miguel Verbitsky, Ph.D., Francesca Lugani, M.D., Ph.D., Roel Sterken, Ph.D., Neal Paragas, Ph.D., Gianluca Caridi, B.S., Alba Carrea, B.S., Monica Dagnino, B.S., Anna Materna-Kiryluk, M.D., Ph.D., Giuseppe Santamaria, Ph.D., Corrado Murtas, M.D., Nadica Ristoska-Bojkovska, M.D., Claudia Izzi, M.D., Ph.D., Nilgun Kacak, M.D.,

Beatrice Bianco, M.D., Stefania Giberti, M.D., Maddalena Gigante, Ph.D., Giorgio Piaggio, M.D., Loreto Gesualdo, M.D., Ph.D., Durdica Kosuljandic Vukic, M.D., Katarina Vukojevic, M.D., Ph.D., Mirna Saraga-Babic, M.D., Ph.D., Marijan Saraga, M.D., Ph.D., Zoran Gucev, M.D., Ph.D., Landino Allegri, M.D., Anna Latos-Bielenska, M.D., Ph.D., Domenica Casu, M.D., Matthew State, M.D., Ph.D., Francesco Scolari, M.D., Roberto Ravazzolo, M.D., Ph.D., Krzysztof Kiryluk, M.D., Qais Al-Awqati, M.B., Ch.B., Vivette D. D'Agati, M.D., Iain A. Drummond, Ph.D., Velibor Tasic, M.D., Ph.D., Richard P. Lifton, M.D., Ph.D., Gian Marco Ghiggeri, M.D., Ph.D., and Ali G. Gharavi, M.D.

The authors' affiliations are as follows: the Divisions of Nephrology (S.S.-C., R.V.S., N.P., K.E.B., S.N.N., B.J.P., P.L.W., M.V., F.L., R.S., N.P., N.K., K.K., Q.A.-A., A.G.G.) and Pediatric Nephrology (P.L.W.) and the Department of Pathology (V.D.D.), Columbia University, and the Department of Medicine, St. Luke's–Roosevelt Hospital Center (S.S.-C.), New York; the Department of Genetics, Howard Hughes Medical Institute, and Yale Center for Mendelian Genomics, Yale University, New Haven, CT (M.C., M.S., R.P.L.); the Department of Biomedical Sciences, Seoul National University College of Medicine, Seoul, South Korea (M.C.); the Division of Nephrology, Dialysis, and Transplantation (M.B., F.L., G.C., A.C., M.D., C.M., G.P., G.M.G.) and Laboratory of Molecular Genetics (G.S., R.R.), Istituto Giannina Gaslini, the Division of Nephrology, Department of Internal Medicine (M.B.), and Dipartimento di Neuroscienze, Riabilitazione, Oftalmologia, Genetica e Scienze Materno Infantili (R.R.), University of Genoa, and IRCCS San Martino-IST (M.B.), Genoa; Cattedra di Nefrologia, Università di Brescia, Seconda Divisione di Nefrologia Azienda Ospedaliera Spedali Civili di Brescia Presidio di Montichiari, Brescia (C.I., F.S.); the Department of Clinical Medicine, Nephrology, and Health Sciences, Unit of Nephrology, University of Parma, Parma (B.B., S.G., L.A.); the Department of Medical and Surgical Sciences, University of Foggia, Foggia (M.G.); the Department of Emergency and Organ Transplantation, University of Bari, Bari (L.G.); and the Division of Nephrology and Dialysis, Hospital of Alghero, Alghero (D.C.) — all in Italy; the Nephrology Division, Massachusetts General Hospital (Y.L., I.A.D.), and Department of Genetics, Harvard Medical School (I.A.D.), Charlestown, MA; University Children's Hospital, Medical School of Skopje, Skopje, Macedonia (V.J.L., N.R.-B., Z.G., V.T.); the Department of Medical Genetics, Poznan University of Medical Sciences, Poznan, Poland (A.M.-K., A.L.-B.); and the Department of Pediatrics, University Hospital of Split (D.K.V., M.S.), and the Department of Anatomy, Histology, and Embryology (K.V., M.S.-B.), School of Medicine (M.S.), University of Split, Split, Croatia.

REFERENCES

1. Loane M, Dolk H, Kelly A, Teljeur C, Greenlees R, Densem J. Paper 4: EUROCAT statistical monitoring: identification and investigation of ten year trends of congenital anomalies in Europe. Birth Defects Res A Clin Mol Teratol 2011;91: Suppl 1:S31-S43.

2. Birth Defects Monitoring Program (BDMP)/Commission on Professional and Hospital Activities (CPHA) surveillance data, 1988–1991. Teratology 1993;48:658-75.

3. Ardissino G, Dacco V, Testa S, et al. Epidemiology of chronic renal failure in children: data from the ItalKid project. Pediatrics 2003;111:e382-e387.

4. Sanna-Cherchi S, Ravani P, Corbani V, et al. Renal outcome in patients with congenital anomalies of the kidney and urinary tract. Kidney Int 2009;76:528-33.

5. Woolf AS, Winyard PJ. Molecular mechanisms of human embryogenesis: developmental pathogenesis of renal tract malformations. Pediatr Dev Pathol 2002; 5:108-29.

6. Weber S, Moriniere V, Knuppel T, et al. Prevalence of mutations in renal developmental genes in children with renal hypodysplasia: results of the ESCAPE study. J Am Soc Nephrol 2006;17:2864-70.

7. Thomas R, Sanna-Cherchi S, Warady BA, Furth SL, Kaskel FJ, Gharavi AG. HNF1B and PAX2 mutations are a common cause of renal hypodysplasia in the CKiD cohort. Pediatr Nephrol 2011;26: 897-903.

8. Sanna-Cherchi S, Caridi G, Weng PL, et al. Localization of a gene for nonsyndromic renal hypodysplasia to chromosome 1p32-33. Am J Hum Genet; 2007; 80:539-49.

9. Weng PL, Sanna-Cherchi S, Hensle T, et al. A recessive gene for primary vesicoureteral reflux maps to chromosome 12p11-q13. J Am Soc Nephrol 2009;20: 1633-40.

10. Boyden LM, Choi M, Choate KA, et al. Mutations in kelch-like 3 and cullin 3 cause hypertension and electrolyte abnormalities. Nature 2012;482:98-102.

11. Sanna-Cherchi S, Burgess KE, Nees SN, et al. Exome sequencing identified MYO1E and NEIL1 as candidate genes for human autosomal recessive steroid-resistant nephrotic syndrome. Kidney Int 2011;80:389-96.

12. Langenau DM, Feng H, Berghmans S, Kanki JP, Kutok JL, Look AT. Cre/lox-regulated transgenic zebrafish model with conditional myc-induced T cell acute lymphoblastic leukemia. Proc Natl Acad Sci U S A 2005;102:6068-73.

13. Sanna-Cherchi S, Kiryluk K, Burgess KE, et al. Copy-number disorders are a common cause of congenital kidney malformations. Am J Hum Genet 2012;91:987-97.

14. Abe G, Ide H, Tamura K. Function of FGF signaling in the developmental process of the median fin fold in zebrafish. Dev Biol 2007;304:355-66.

15. Griffin KJ, Kimelman D. Interplay between FGF, one-eyed pinhead, and T-box transcription factors during zebrafish posterior development. Dev Biol 2003;264: 456-66.

16. Nissen RM, Yan J, Amsterdam A, Hopkins N, Burgess SM. Zebrafish foxi one modulates cellular responses to Fgf signaling required for the integrity of ear and jaw patterning. Development 2003; 130:2543-54.

17. Bates CM. Role of fibroblast growth factor receptor signaling in kidney development. Am J Physiol Renal Physiol 2011; 301:F245-F251.

18. Corson LB, Yamanaka Y, Lai KM, Rossant J. Spatial and temporal patterns of ERK signaling during mouse embryogenesis. Development 2003;130:4527-37.

19. Schedl A. Renal abnormalities and their developmental origin. Nat Rev Genet 2007;8:791-802.

20. Sanna-Cherchi S, Caridi G, Weng PL, et al. Genetic approaches to human renal agenesis/hypoplasia and dysplasia. Pediatr Nephrol 2007;22:1675-84.

21. Barak H, Huh SH, Chen S, et al. FGF9 and FGF20 maintain the stemness of nephron progenitors in mice and man. Dev Cell 2012;22:1191-207.

22. Poladia DP, Kish K, Kutay B, et al. Role of fibroblast growth factor receptors 1 and 2 in the metanephric mesenchyme. Dev Biol 2006;291:325-39.

23. Guillemot F, Zimmer C. From cradle to grave: the multiple roles of fibroblast growth factors in neural development. Neuron 2011;71:574-88.

24. Zhao H, Kegg H, Grady S, et al. Role of fibroblast growth factor receptors 1 and 2 in the ureteric bud. Dev Biol 2004; 276:403-15.

25. Zha J, Zhou Q, Xu LG, et al. RIP5 is a RIP-homologous inducer of cell death. Biochem Biophys Res Commun 2004;319: 98-303.

Copyright © 2013 Massachusetts Medical Society.

629